Indian J. Phys. **78** (11), 1187-1192 (2004)

AN INTERNATIONAL JOURNAL
IJP

Impact of high energy radiation effects on *N*-channel MOSFETs

A P Gnana Prakash[1*], John D Cressler[1], S C Ke[2] and K Siddappa[3]

[1]School of Electrical and Computer Engineering, Georgia Institute of Technology, TSRB, 85 fifth street, Atlanta-30308, GA, USA

[2]Department of Physics, National Dong Hwa University, Shou-Feng, Hualien-974-01, Taiwan, Republic of China

[3]Microtron Center, Department of Physics, Mangalore University, Mangalagangotri, Mangalore-574 199, Karnataka, India

E-mail gprakash@ece.gatech.edu

Received 30 October 2003, accepted 9 September 2004

Abstract The effect of 30 MeV Li^{3+} ion and 8 MeV electron irradiations on the threshold voltage (V_{TH}), the voltage shift due to interface trapped charge (ΔV_{Nit}), the voltage shift due to oxide trapped charge (ΔV_{Not}), the density of interface trapped charge (ΔN_{it}), the density of oxide trapped charge (ΔN_{ot}) and the drain saturation current ($I_{D\,Sat}$) were studied as a function of fluence. The considerable increase in the ΔN_{it} and ΔN_{ot}, and decrease in V_{TH} and $I_{D\,Sat}$ were observed in both types of irradiations. The observed difference in the properties of Li^{3+} ion and electron irradiated MOSFETs are interpreted on the basis of energy loss process associated with the type of radiation. The study showed that the 30 MeV Li^{3+} ion irradiation produce more damage when compared to the 8 MeV electron irradiation because of the higher electronic energy loss value.

Keywords · Trapped charge, MOSFET, ion irradiation, electron irradiation, voltage shift

PACS Nos. 71.30.+h, 71.55.-h, 72.20.Jv

1. Introduction

It has been of long standing concern that ionizing radiation will degrade the metal oxide semiconductor field effect transistor (MOSFET) performance and eventually make the device malfunction. This degradation is related to the radiation-induced oxide charge build-up in the oxide layer and interface state generation at the silicon/silicon dioxide (Si/SiO_2) interface [1-4]. The ionizing radiation generates electron-hole pairs when incident on the MOS device. The electron being quite mobile in SiO_2 and are quickly swept out whereas holes undergo a slow dispersive transport towards the Si/SiO_2 interface where they get trapped in deep hole traps. This positive charge accumulation in the oxide, produces shift in the flat band, midgap and threshold voltage of the MOS transistors. Secondary effects in the MOS transistors decrease in the transconductance and increase in the source to drain leakage current. Thus, ionization damage produced in the gate oxide and the field oxide is the cause in the degradation in the above properties of MOS transistors [5-9].

The most critical parameters of MOSFET in radiation environment is the threshold voltage (VTH) [10,11]. The shift in VTH (DVTH) can result in the loss of ability to turn the MOSFET on or off, a lack of current drive and a leakage current. The radiation induced DVTH is caused by the trapping of charge in the oxide and generation of interface states. Recent investigations show that the interface traps build-up may occur because of the motion of hydrogen-related species (*e.g.* proton) released during irradiation and can be retarded by interactions with oxygen vacancies in the SiO_2 [12]. Poindexter *et al* [13] have reported that the radiation induced hole trap is an E' defect (a trivalent silicon center in SiO_2 with oxygen vacancy) and the interface trap is a Pb defect (a trivalent silicon center at the Si/SiO_2 interface). These are the only point defects known to play an important role in the degradation of MOS devices under irradiation conditions [14]. The annealing of oxide and interface-trapped charge were studied by many researchers and several models were proposed at various elevated temperatures and at different electrical stress [15,16].

*Corresponding Author

Although an extensive effort was made to understand the influence of various kinds of radiation such as X-rays, Co-60 gamma rays and neutrons on the electrical characteristics of the MOSFETs, very little information is available on the effect of high-energy heavy ion and electron irradiation. Therefore in the present work, we investigated the total dose/fluence response of the *N*-channel MOSFETs for the 30 MeV Li^{3+} ion and the 8 MeV electron irradiations. The overall objective of the work reported here is to provide comparative studies of the 30 MeV Li^{3+} ion and 8 MeV electron irradiations effect on the ΔV_{TH}, ΔN_{it}, ΔN_{ot} and the $I_{D\,Sat}$.

2. Experiment

In the present work two serially connected *N*-channels with independent dual gate depletion MOSFETs (BEL 3N187) with isolated silicon substrate (<100> 4-11 ohm cm of thickness ~ 650 μm) and the gate oxide thickness (SiO_2) ≈ 750 ± 50 °A are investigated. The gate metal (Al) thickness is ≈ 1.2 μm while the device channel size is ≈1.2 μm x 5 μm. The cross sectional view of the *N*-channel MOSFET is shown in Figure 1. The *N*-channel MOSFETs were exposed to 30 MeV Li^{3+} ions at the 15 UD 16 MV Pelletron Tandem Van de Graff Accelerator at Nuclear Science Centre (NSC), New Delhi, India [17]. The MOSFETs were irradiated with ion fluence ranging from 1×10^{11} to 5×10^{13} ions/cm^2 at 300 K in an experimental chamber of diameter 1.5 m maintained at 10-7 mbar vacuum. The typical beam current while irradiating the MOSFETs was around 2-4 particle nanoamperes (pnA). The fluence on the sample kept in cylindrical secondary electron suppressed geometry was estimated by integrating the total charge accumulated on the sample using a current integrator and then counting by a scalar meter. The ion beam was scanned over the samples in an area of 10 mm × 10 mm by magnetic scanner in order to get uniform fluence. The 8 MeV electron at 4-12 MeV Variable Energy Microtron Center [18] in the fluence range from 1.6×10^{12} to 1.3×10^{14} electrons/cm^2 in open air at room temperature. In both cases, all devices were irradiated with gate bias (V_{GS}) = +3 V.

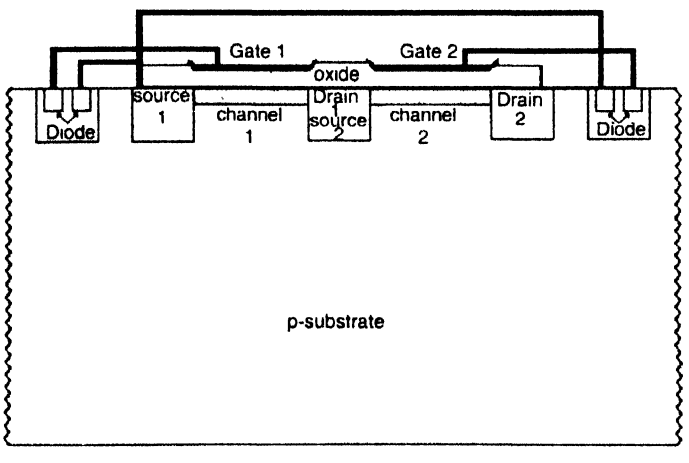

Figure 1. The cross sectional view of the *N*-channel MOSFET.

The electrical characterization of the devices before and after irradiation were performed using computer interfaced Keithley 236 source measure units with trigger controller and the test set up is shown in the Figure 2. The threshold voltage (V_{TH}) was determined from the drain current versus gate voltage (I_D-V_{GS}) characteristics. Among the several methods available to measure the threshold voltage (V_{TH}), one method is to choose a current level and define the gate voltage (V_{GS}) required to produce that drain-source current (I_D) [19]. The drain saturation current ($I_{D\,Sat}$) was determined from drain to source voltage and drain current (V_{DS} – I_D) characteristics measured at zero gate bias (V_{GS} = 0 V). While measuring the threshold voltage (V_{TH}) and drain saturation current ($I_{D\,Sat}$), equal voltage was applied to the both gates.

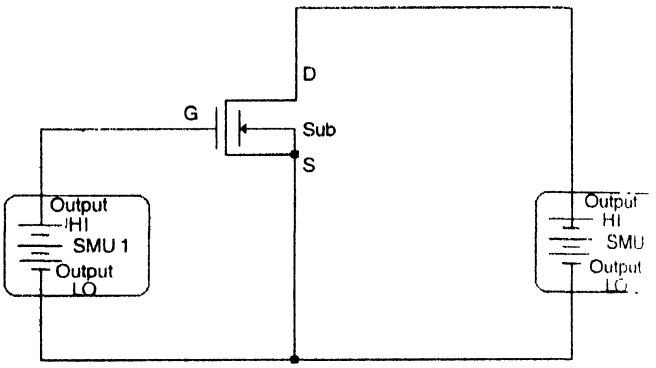

Figure 2. Keithley Source Measure Units (SMUs) to measure electri characteristics of *N*-channel MOSFET

3. Results and discussion

To understand the observed modifications in the irradiated devices, it is important to analyze the effect of irradiation on the device structure and role of the associated energy lo mechanisms. It is well established that when high-energy ion passes through a material, it looses its energy *via* two processes namely electronic (*e*) excitations (electronic energy loss, $\langle dE/dx \rangle e$) and direct nuclear (*n*) collisions with the target atoms (nuclear energy loss, $\langle dE/dx \rangle n$). The nuclear energy loss is much smaller than the electronic energy loss (three orders of magnitude) in a material due to smaller elastic scattering cross section. Therefore, all the energy deposited to the material is mainly due to the electronic energy loss process during its early passage into the material. The nuclear energy loss becomes dominant near the end of the ion range and this produces point defects and the collision cascades. We have used SRIM-2003 [20] simulation program to estimate the value of $\langle dE/dx \rangle e$, $\langle dE/dx \rangle n$ and range of the 30 MeV Li^{3+} ions in the Metal Oxide Semiconductor (MOS) device structure and given in the Table 1. From the SRIM calculations, it is clear that the ions pass through the aluminium gate, SiO_2 layer and finally get implanted deep inside the silicon *p*-substrate at a depth of around 132 μm from the surface. When MOS devices exposed to 30 MeV Li^{3+}

Table 1 The energy loss and range of 30 MeV Li^{3+} ions in Metal Oxide Semiconductor (MOS) structure.

Source	Energy (MeV)	LET in MeV cm²/g			Range in		
		Al	Si	SiO_2	Al	Si	SiO_2
Electron	8	1 97	1 92	1.88	1.81 cm	1 86 cm	1 99 cm
Li ions	30	585 9	598 3	634 2	116 12 mm	131 56 mm	123 35 mm

ions, these ions pass through the SiO_2 layer and they deposit higher energy through electronic excitations. These high energy ions which will produce ionization or breaking bonds and displacement of atoms along its path during irradiation process. From the SRIM simulation data, it is revealed that each ion can create around 750 vacancies before it stops deep inside the silicon substrate. The energy loss of 8 MeV electrons is only 1 92 MeV cm²/g in silicon since the range of electron is 1.86 cm in silicon. When the 30 MeV Li^{3+} ion and 8 MeV electron pass through the SiO_2 layer, they deposit higher energy through electronic excitations, which will produce ionization or breaking bonds and displacement of atoms along its path. In the MOSFETs, the role of Si/SiO_2 interface is very important in determining the device performance. Some of the radiation-induced electron-hole pairs are quickly undergo recombination and are not available for any further radiation effect and some of the positively charged holes make slow dispersive transport towards the Si/SiO_2 interface where they get trapped in deep hole traps. The microscopic origin of the dispersive transport is likely to be multiple trapping and detrapping of the holes or hopping of the holes through shallow traps. This results in additional oxide charges (Not) and reduces the threshold voltage (VTH). These Not are located at or near the Si/SiO_2 interface and are immobile under applied electric field. The electron trapping in SiO_2 is negligible because the capture cross section of electron traps is very small (by a factor of 10^4) when compared to the hole traps.

To determine the threshold voltage (VTH), we studied the sub-threshold behaviour of irradiated transistors as a function of fluence and plots for the 30 MeV Li^{3+} ions and 8 MeV electron irradiated MOSFETs are shown in Figures 3a, 3b respectively.

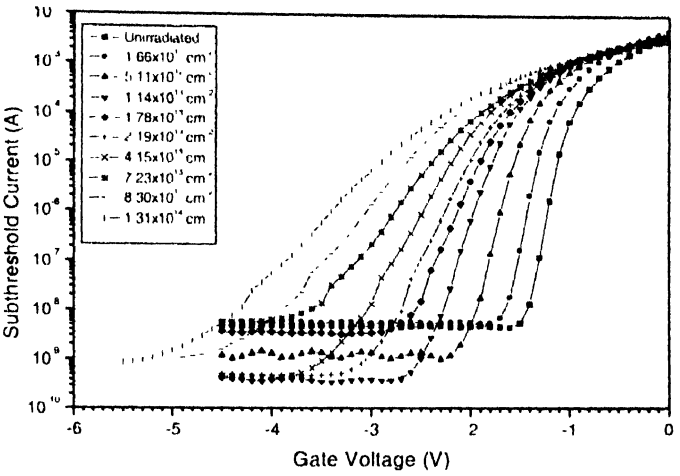

Figure 3b Sub-threshold current curves for *N* channel MOSFET before and after 8 MeV electron irradiation

The V_{TH} for these devices is defined as the negative gate voltage for which the drain current becomes 1 μA ($V_{TH} \equiv V_{GS} @ I_D = 1\ \mu A$). Figure 4 shows the variation in V_{TH} with respect to fluence for both the Li^{3+} ion and electron-irradiated MOSFETs. For the transistors irradiated with the Li^{3+} ion with fluence up to 1×10^{13} cm^{-2}, the V_{TH} decreased from −1.19 to −4.52 V and that irradiated with the electron with fluence up to 1.31×10^{14} cm^{-2}, the VTH decreased from −1.19 to −3.39 V. The $I_D - V_{DS}$ characteristic curves for 30 MeV Li^{3+} ion and 8 MeV electron-irradiatiated MOSFETs are shown in Figures 5a, 5b respectively. To illustrate in a better way, $I_{D,Sat}$ was extracted from the $I_D - V_{DS}$ curves at $V_{DS} = 3$ V and is shown in Figure 6 for both types of irradiations. It can be seen from the figure that

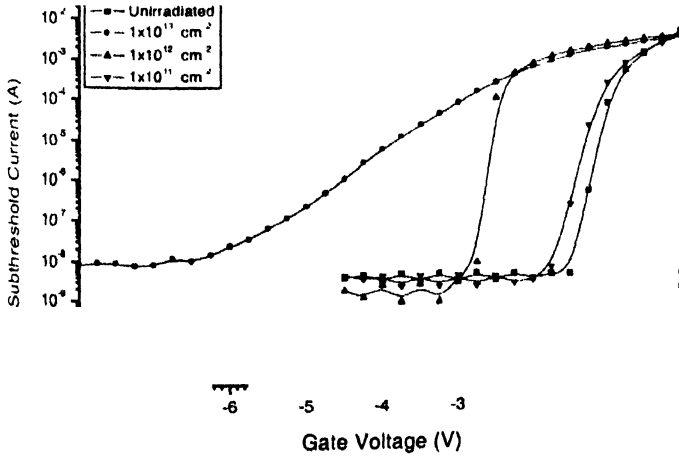

Figure 3a. Sub-threshold current curves for *N*-channel MOSFET before and after 30 MeV Li^{3+} ion irradiation.

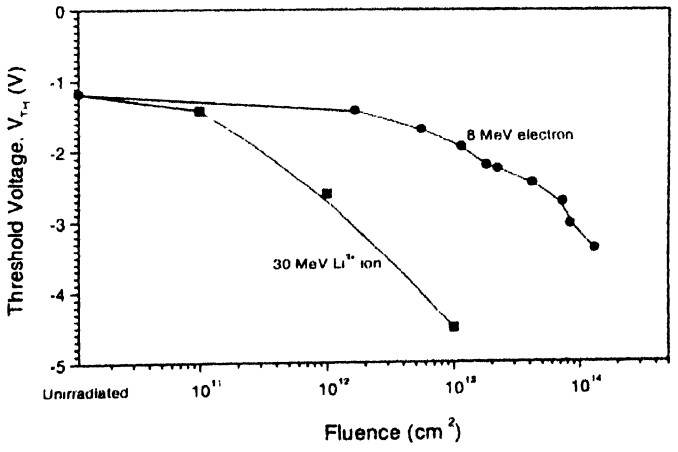

Figure 4 Variation in the V_{TH} before and after 30 MeV Li^{3+} ion and 8 MeV electron irradiation.

$I_{D\ Sat}$ decreased by an order of magnitude for ion-irradiated MOSFETs and slight decrease is evident in the case of electron-irradiated MOSFETs. From Figure 6, it can be observed that

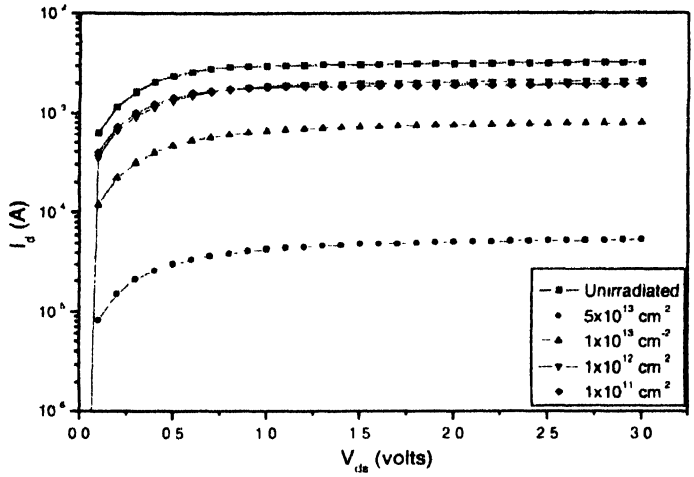

Figure 5a. $I_D - V_{DS}$ characteristics before and after 30 MeV Li^{3+} ion irradiation (at $V_{GS} = 0$ V)

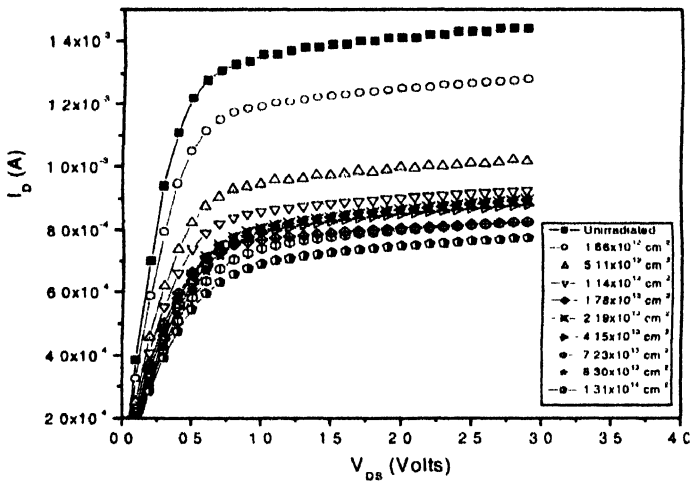

Figure 5b. $I_D - V_{DS}$ characteristics: before and after 8 MeV electron irradiation (at $V_{GS} = 0$ V).

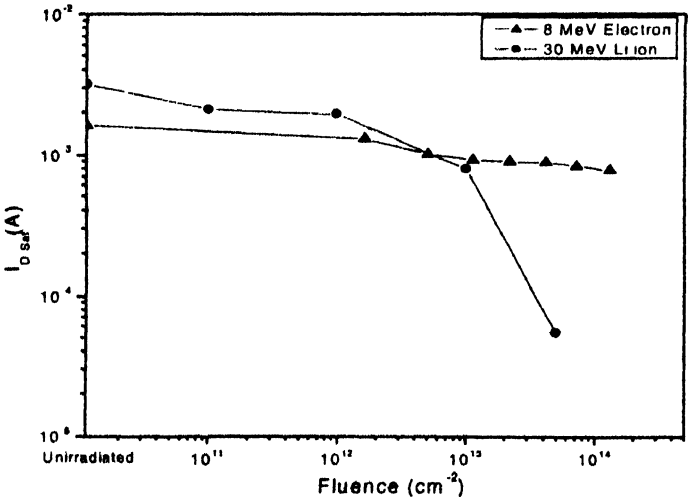

Figure 6. Variation in the drain saturation current, $I_{D\ Sat}$ for the 30 MeV Li^{3+} ion and the 8 MeV electron irradiated MOSFETs (at $V_{GS} = 0$ V).

$I_{D\ Sat}$ decreased from 3.18 mA to 0.0536 mA for the 30 MeV Li^{3+} ion-irradiated MOSFET after a total fluence of 5×10^{13} cm^{-2}. In case of 8 MeV electron-irradiated MOSFET, ID Sat decreased from 1.69 mA to 0.776mA after a total fluence of 1.31×10^{14} cm^{-2}. The decrease in $I_{D\ Sat}$ may be due to the Coulomb scattering between the radiation induced interface-trapped charge and free carriers in the channel. Because of the large difference in the electronic energy loss between the 30 MeV Li^{3+} ion and the 8 MeV electron, the energy deposition is more for the Li^{3+} ion and therefore the damage is more.

The net threshold voltage shift (ΔV_{TH}) and contribution to that shift due to the interface traps (ΔV_{Nit}) and the trapped oxide charge (ΔV_{Not}), was calculated from the sub-threshold measurements using the technique proposed by McWhorter and Winokur [21]. From this technique, it is possible to split the threshold voltage shift (ΔV_{TH}) into a contribution due to interface-trapped charge (ΔV_{Nit}) and a contribution due to trapped oxide charge (ΔV_{Not}), where $\Delta V_{TH} = \Delta V_{Nit} + \Delta V_{Not}$ from sub-threshold current measurements. The high energy radiation introduces both interface traps and trapped oxide charge which in turn, causes a shift in the threshold voltage. The first step in the analysis is to determine the currents at Si surface potentials corresponding to threshold and midgap for each curve. The sub-threshold current for a transistor in saturation, can be calculated as a function of surface band bending using the formula [21]:

$$I_d = \sqrt{2} C_m (qN_A L_B/\beta)(n_i/N_A)^2 \exp(\beta\phi_s)(\beta\phi_s)^{-1/2}$$

where ϕ_s is the band bending at the surface, N_A is the channel doping, n_i is the intrinsic carrier concentration, L_B is the Debey length given by $L_B = \left[\varepsilon_s/(\beta qN_A)\right]^{1/2}$, $\beta = q/kT$, and C_m is $\mu(W/2L)$.

This technique involves measuring increments or shifts in the sub-threshold current slopes and is not sensitive to details of the actual doping profile in the depletion layer. C_m is determined from the slope of a plot of the square root of drain current *versus* gate voltage in saturation, since

$$I_d = C_m C_{ox} \left(V_g - V_{thex}\right)^2 \tag{2}$$

with V_{thex} being the extrapolated threshold voltage. After C_m is determined for each curve, it is then possible to calculate the threshold and midgap currents. The threshold current is simply the current associated with V_{thex}. The midgap current is defined as the current which occurs when the bands are bent at the surface by an amount ϕ_b, where $\phi_b = (kT/q)\ln(N_A/N_i)$. Since the midgap current tends to be in the range of 0.01-0.1 pA, it is generally necessary to linearly extrapolate the lower position of the sub-threshold curve down to this curve level.

With the threshold and midgap currents marked on each of the curves, it is now possible to determine shifts in the threshold voltage (ΔV_{th}) and midgap voltage (ΔV_{mg}) at each radiation level. The interface traps in the upper half of the band gap are generally believed to be acceptors, while interface traps in the lower half of the band gap are donors. Therefore, as the bands are bent from midgap to threshold, an increased number of acceptor interface traps fall bellow the Fermi level and become negatively-charged. This has the effect of stretching out the sub-threshold current curve between midgap and threshold. We define the stretch out voltage V_{so} to be the voltage difference between the midgap and threshold points and is given by

$$V_{so} = V_{th} - V_{mg} \,. \tag{3}$$

The shift in the threshold voltage due to interface traps is therefore the difference in the stretchout voltage on respective sub-threshold current curves *i.e.*

$$\Delta V_{Nit} = (V_{so})_2 - (V_{so})_1 \tag{4}$$

where the labels 2 and 1 refer to sub-threshold current curves at different radiation levels. Once the threshold voltage shift due to interface traps is known, the increase in the number of interface traps can be determined by

$$\Delta N_{it} = \Delta V_{Nit}\, C_{ox}/q \,. \tag{5}$$

ΔN_{it} (cm^{-2}) represents the increase in the total number of interface traps between midgap and threshold; C_{ox} is the capacitance of the oxide per unit area and is given by $C_{ox} = \epsilon_{ox}/t_{ox}$, with t_{ox} being the thickness of the gate oxide. This derivation is based on n assumption of no lateral non-uniformities.

The contribution of trapped oxide charge to the threshold shift is independent of gate bias and simply translates an entire sub-threshold current curve to the left (for positive trapped holes created following irradiation). Based on the above model of interface traps, when the bands are bent by an amount ϕ_b (midgap condition), the donor traps fall below the Fermi level, and the acceptor traps fall above the Fermi level. This means the interface traps are uncharged. Therefore, the shift between sub-threshold curves at the midgap voltage represent the shift due to trapped charge in the oxide *i.e.*

$$\Delta V_{Not} = (V_{mg})_2 - (V_{mg})_1 \,. \tag{6}$$

Once ΔV_{Not} is known, the increase in the number of trapped charges in the oxide can be calculated by

$$\Delta N_{ot} = \Delta V_{Not}\, C_{ox}/q \,. \tag{7}$$

This technique provides an accurate method of determining the build-up of interface traps and trapped-oxide charge without sophisticated measurements or complicated analysis.

The variation of the ΔN_{it} and the ΔN_{ot} as a function of fluence are shown in Figures 7, 8 respectively for the devices irradiated with the 30 MeV Li^{3+} ion and 8 MeV electron. For the Li^{3+} ion-irradiated MOSFET, the ΔN_{it} increased from 6.192×10^{10} to 1.365×10^{12} cm^{-2} and the ΔN_{ot} from 1.354×10^{11} to 2.324×10^{12} cm^{-2}. In the case of electron irradiation, the ΔN_{it} increased from 3.744×10^{10} to 8.784×10^{11} cm^{-2} and the ΔN_{ot} also increased from 9.792×10^{10} to 1.506×10^{12} cm^{-2}. However, the increase in ΔN_{it} and ΔN_{ot} are much higher for the 30 MeV Li^{3+} ion compared to 8 MeV electron-irradiated MOSFETs.

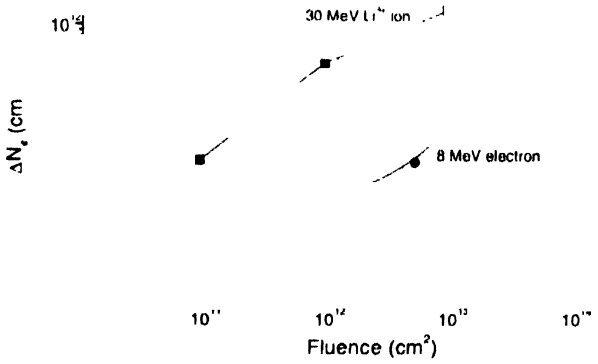

Figure 7 Variation in the ΔN_{it} after 30 MeV Li^{3+} ion and 8 MeV electron irradiation.

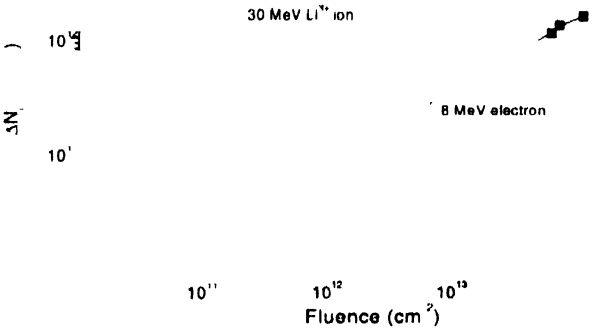

Figure 8 Variation in the ΔN_{ot} after 30 MeV Li^{3+} ion and 8 MeV electron irradiation

4. Conclusions

In this work, we observed that the V_{TH} of MOS devices have been decreased significantly after the 30 MeV Li^{3+} ion and the 8 MeV electron irradiations. The conduction mechanisms of the source to drain junction were strongly affected by the radiation-induced trapped charge and significant decrease in the $I_{D\,Sat}$ was observed. The interface trapped charge (ΔN_{it}) and oxide trapped charge (ΔN_{ot}) were calculated from the sub-threshold measurements and ΔN_{ot} was found to be higher compared to ΔN_{it} after exposure to both 30 MeV Li^{3+} ions and 8 MeV